AIAA 80-0010R

Compressibility Effects on Dynamic Stall of an NACA 0012 Airfoil

N. L. Sankar* and Y. Tassa†
Lockheed-Georgia Company, Marietta, Ga.

Abstract

DYNAMIC stall of an NACA 0012 airfoil for laminar flow conditions was studied by solving the compressible Navier Stokes equations in a body-fitted coordinate system. The compressibility effects on the dynamic stall were studied by computing the flow properties at Mach numbers 0.2 and 0.4 while freezing the chord Reynolds number and the reduced frequency at 5000 and 0.5, respectively. The numerical results indicate that compressibility has an inhibiting effect on the formation and growth of the leading-edge vortex. During the upstroke motion, prior to the formation of vortex, the lift and moment coefficients are consistently higher at the higher Mach number. Also, during the downstroke motion, the numerical results predict that the spilled vortex is convected downstream at a greater speed for the higher Mach number case.

Contents

The unsteady compressible Navier Stokes equations were cast in a strong conservation form in a body-fitted coordinate system. A modified form of Beam-Warming algorithm[1] as described by Steger[2] was developed and used to solve the governing equations.

The reliability of the numerical procedure was established by studying two test cases, one involving laminar separated flow about a circular cylinder at a Reynolds number of 40 based on diameter, and the second case involving the static stall of a 9% airfoil at 15 deg angle of attack for a Reynolds number and Mach number of 10^3 and 0.2, respectively (see Ref. 3).

In the present paper the numerical approach was applied to obtain the dynamic stall characteristics of a modified NACA 0012 airfoil. In order to obtain quantitative comparison with well-documented data the airfoil shape studied in Ref. 4 was used. A conformal mapping of an O-Grid in the physical plane coupled with a clustering of the grid lines near the airfoil to resolve the viscous region was used.

Three cases are presented in Table 1. Only cases 1 and 2 are discussed here; the reader interested in case 3 is referred to Ref. 3.

A comparison of the numerical results with the incompressible case of Ref. 4 is given in Table 2. It appears that the present results of case 1 compare reasonably well with the results of Ref. 4, except during portions of the downstroke motion. Water tunnel experiments, as presented in Ref. 4, indicate that the flow becomes turbulent during the downstroke. Thus, neither the present results nor the results of Ref. 4 may be valid for the entire downstroke motion.

The lift and moment hysteresis loops for case 1 and case 2 are shown in Figs. 1-4. The following features distinguish the two cases from one another. 1) During the upstroke motion, the lift drag and moment coefficients at Mach number of 0.4 are consistently higher than the corresponding values for Mach of 0.2, which in turn are consistently higher than the values presented in Ref. 4 using the incompressible Navier-Stokes equations. This trend continues until the leading-edge vortex begins to form. It appears that these three sets of results may be collapsed into a single curve using a suitable empirical relationship patterned in the spirit of the Prandtl-Glauert relationship. 2) The leading edge vortex begins to form during the upstroke at an angle of attack of 18.6 deg for case 1 and at an angle of attack of 19.3 deg for case 2. In addition, the pressure suction peaks associated with this vortex are higher for the 0.2 Mach number case compared to the 0.4 Mach number case. Thus, compressibility appears to

Table 1 Summary of flow conditions studied

Case	M_∞	N_R	Reduced frequency	$\alpha(t)$, deg
1	0.2	5×10^3	1.0	$10\,[1-\cos(t)]$
2	0.4	5×10^3	1.0	$10\,[1-\cos(t)]$
3	0.4	1×10^4	0.5	$10\,[1-\cos(t/2)]$

Table 2 Comparison of compressible and incompressible Navier-Stokes results for the dynamic stall of an NACA 0012 airfoil; Reynolds number = 5000, reduced frequency = 1.0

α, deg	M_∞	C_L	C_M	C_D	Method
0	Incomp.	0	0	0.0534	Ref. 4
	0.2	0	0	0.0579	Present
	0.4	0	0	0.0612	
14.86	Incomp.	1.228	−0.0608	0.252	Ref. 4
	0.2	1.241	−0.0709	0.271	Present
	0.4	1.285	−0.0782	0.303	
18.5	Incomp.	1.385	−0.0473	0.336	Ref. 4
	0.2	1.4346	−0.0623	0.3532	Present
	0.4	1.457	−0.0610	0.3940	
20.0	Incomp.	1.278	−0.0036	0.367	Ref. 4
	0.2	1.506	−0.0804	0.444	Present
	0.4	1.486	−0.0671	0.489	
19.76	Incomp.	1.489	−0.109	0.478	Ref. 4
	0.2	1.478	−0.112	0.482	Present
	0.4	1.444	−0.0724	0.486	
17.47	Incomp.	0.970	0.0228	0.335	Ref. 4
	0.2	1.180	−0.104	0.351	Present
	0.4	1.296	−0.133	0.434	
11.36	Incomp.	0.846	−0.133	0.227	Ref. 4
	0.2	0.855	−0.164	0.204	Present
	0.4	1.030	−0.254	0.288	
4.78	Incomp.	0.199	−0.102	0.162	Ref. 4
	0.2	−0.093	−0.107	0.119	Present
	0.4	−0.067	−0.001	0.169	
1.82	Incomp.	0.0167	−0.0114	0.110	Ref. 4
	0.2	−0.562	0.1184	0.110	Present
	0.4	−0.429	0.0794	0.116	

Presented as Paper 80-0010 at the AIAA 18th Aerospace Sciences Meeting, Pasadena, Calif., Jan. 14-16, 1980; submitted March 7, 1980; synoptic received Aug. 29, 1980; revision received Dec. 9, 1980. Full paper available from AIAA Library, 555 W. 57th St., New York, N. Y. 10019. Price: Microfiche, $3.00; hard copy, $7.00.

*Scientist Associate, Advanced Flight Sciences Dept. Member AIAA.

†Senior Research Scientist, Advanced Flight Sciences Dept. Member AIAA.

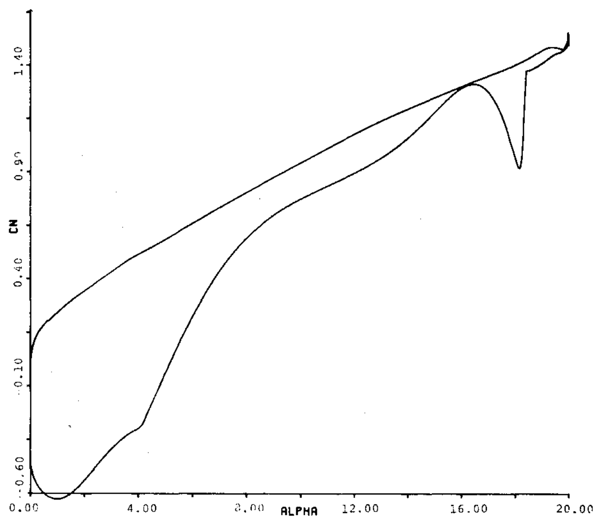

Fig. 1 Lift hysteresis characteristics for case 1; Reynolds number = 5000, Mach number 0.2, reduced frequency based on chord 1.0.

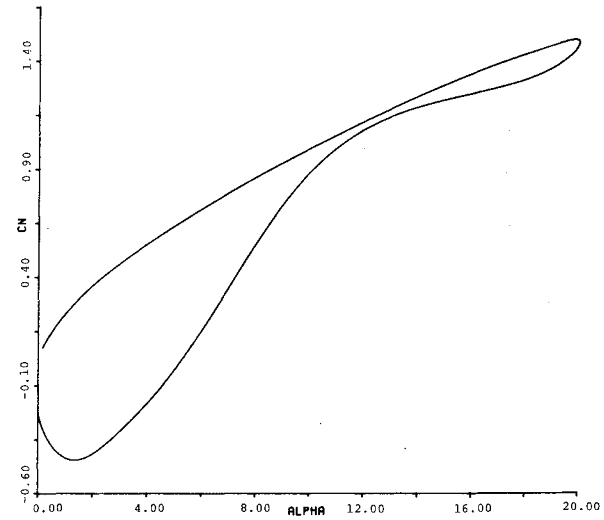

Fig. 3 Lift hysteresis characteristics for case 2; Reynolds number = 5000, Mach number 0.4, reduced frequency based on chord 1.0.

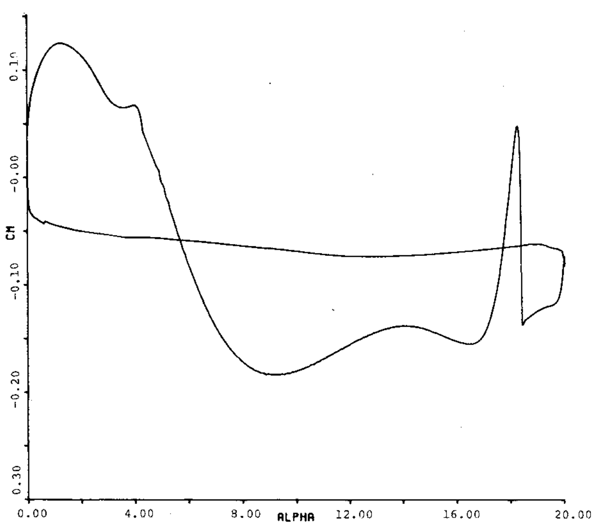

Fig. 2 Moment hysteresis characteristics for case 1.

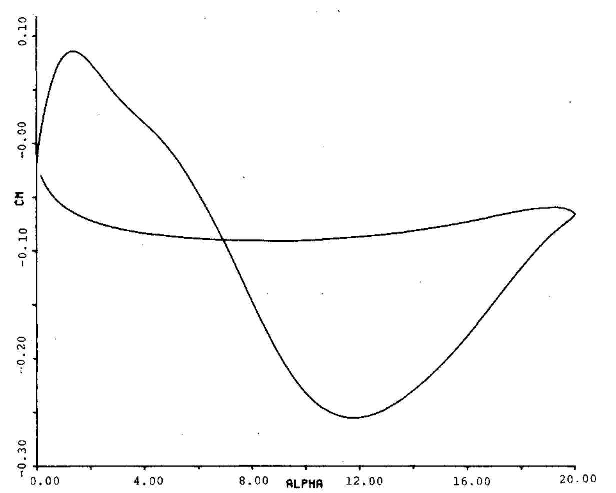

Fig. 4 Moment hysteresis characteristics for case 2.

inhibit the formation and growth of the leading-edge vortex. 3) The convection speed of the spilled vortex has been computed for both cases by tracing the motion of the suction peaks over the upper surface and also from the constant vorticity contours. It appears that the spilled vortex is convected at about 0.24 times the freestream velocity for case 1 and at about 0.32 times the freestream velocity for case 2.

From the preceding observations it is apparent that compressibility has significant effects on the dynamic stall phenomenon. Clearly additional computations of the type reported herein are needed to completely validate the effect of compressibility on dynamic stall. However, because of the quantitative correspondence that we have been able to obtain between the two cases and that of Ref. 4, we feel that our observation of compressibility effects on dynamic stall are at least qualitatively correct.

References

[1]Beam, R., and Warming, R. F., "An Implicit Factored Scheme for the Compressible Navier-Stokes Equations," *AIAA Journal*, Vol. 16, April 1978, pp. 393-402.

[2]Steger, J. L., "Implicit Finite Difference Simulation of the Flow about Arbitrary Two-Dimensional Geometries," *AIAA Journal*, Vol. 16, July 1978, pp. 679-686.

[3]Sankar, N. L. and Tassa, Y., "Reynolds Number and Compressibility Effects on Dynamic Stall of a NACA 0012 Airfoil," AIAA Paper 80-0010, Jan. 1980.

[4]Mehta, U. B., "Dynamic Stall of an Oscillating Airfoil," AGARD Meeting on Unsteady Aerodynamics, Ottawa, Paper 23, AGARD CP 227, Sept. 1977.